We are IntechOpen,
the world's leading publisher of
Open Access books
Built by scientists, for scientists

4,800
Open access books available

122,000
International authors and editors

135M
Downloads

Our authors are among the

154
Countries delivered to

TOP 1%
most cited scientists

12.2%
Contributors from top 500 universities

CLARIVATE ANALYTICS
BOOK CITATION INDEX
INDEXED

WEB OF SCIENCE™

Selection of our books indexed in the Book Citation Index
in Web of Science™ Core Collection (BKCI)

Interested in publishing with us?
Contact book.department@intechopen.com

Renewable Energy Microgrid Design for Shared Loads

Ibrahim Aldaouab and Malcolm Daniels

Additional information is available at the end of the chapter

Abstract

Renewable energy resource (RER) energy systems are becoming more cost-effective and this work investigates the effect of shared load on the optimal sizing of a renewable energy resource (RER) microgrid. The RER system consists of solar panels, wind turbines, battery storage, and a backup diesel generator, and it is isolated from conventional grid power. The building contains a restaurant and 12 residential apartments. Historical meter readings and restaurant modeling represent the apartments and restaurant, respectively. Weather data determines hourly RER power, and a dispatching algorithm predicts power flows between system elements. A genetic algorithm approach minimizes total annual cost over the number of PV and turbines, battery capacity, and generator size, with a constraint on the renewable penetration. Results indicate that load-mixing serves to reduce cost, and the reduction is largest if the diesel backup is removed from the system. This cost is optimized with a combination of particle swarm optimization with genetic-algorithm approach minimizes total annual cost over the number of solar panels and micro-turbines, battery capacity, and diesel generator size, with a constraint on the renewable penetration. Results indicate that load-mixing serves to reduce cost, and the reduction is largest if the diesel backup is removed from the system.

Keywords: renewable energy system, load profile, PV, wind turbine, battery, loads shared

1. Introduction

1.1. Distributed electricity generation

Electrical power is historically generated at a few large power stations and transmitted over long distances to end users. However, in recent years, there is an increase in decentralized or distributed electric power generation, where the power is produced and used at the same

location [1]. Often, this decentralized power is produced with renewable energy technologies, such as wind and solar, due to the decreasing costs of these technologies [1].

There are many advantages to a power distribution system that relies on many small generation facilities rather than a few large power plants. Transmitting power over long distances is inefficient and requires expensive infrastructure. Smaller facilities that are close to where the power is used can provide higher quality power, with fewer blackouts and a more steady voltage. Since many of the small generating stations are natural gas powered or powered with renewable sources, there is less pollution than large plants that often run on coal. Finally, a distributed energy generation model is more secure than a centralized model.

The challenge to expanding distributed electricity generation is partly economic and partly technical. The capital costs for building a small-scale facility is large relative to the power it can produce. Many renewable technologies produce irregular power that varies with the weather, and this power is difficult to incorporate into the grid [2].

1.2. Motivation for expanding distributed generation

Increasing attention is given to designs for integrating renewable energy with traditional power to satisfy electrical loads from individual or multiple buildings. Research in this area is driven by several factors. First, costs for photovoltaic (PV) panels and wind micro-turbines (MT) are steadily dropping, along with battery energy storage systems (BESS). For example, the reported cost of installed solar PV systems fell by an average of 6–12% per year from 1998 to 2014, depending on the scale of the system [3]. Similarly, the price of wind power is dropping significantly, as more turbines are brought online, and currently about 5% of the energy requirements for the United States is supplied through wind power. In the previous decade, more than two-thirds of all wind installations in the United States have been small- or mid-sized wind turbines [4]. Battery storage has also dropped to a level of about $100 per kWh of capacity [5]. Another motivating factor is the various grid-pricing structures available, which often create an incentive for using less power at certain times of the day or making the overall electrical demand more uniform. Microgrids can achieve this, reducing the cost of grid electrical power.

In addition to economic motivation, there is increased recognition of the damage to the environment due to CO_2 emission from traditional power generation. The benefit of using RER microgrids for buildings is the potential reduction in carbon and other pollutants because buildings consume over 40% of end-use energy worldwide [6]. In order to address the problem of efficient building energy use and to reduce pollution in buildings, the United States has set a zero net energy target on 50% of commercial buildings by 2040 and on all commercial buildings by 2050 [6]. A zero net energy building is one that produces some renewable energy on-site, such that the building sometimes uses grid power and at other times produces extra renewable power. The average amount of renewable power produced annually is the same as the building's average annual consumption.

Finally, another advantage for microgrids is the improved reliability that they offer. There are multiple sources of power in a microgrid, such that there is less chance of a complete power outage.

1.3. Problem statement

Several studies consider the optimal design and sizing of the RER system for residential or commercial building individually [7, 8]. The RER microgrid design in this work is applied to a mixed commercial and residential building. Residential loads peak in the evening and early morning times, whereas commercial loads peak in the daytime. A shared residential and commercial load therefore has the potential to be more uniform than one or the other alone. A uniform load is easier to efficiently match to the RER supply, and it may also help lower the grid power costs. This chapter studies the effect of combining loads for an RER microgrid on the full cost of the microgrid. The size of the RER system partly depends on the shape of the load profile, such that irregular profiles require larger RER systems than smooth profiles. For example, an irregular load profile requires more energy storage to satisfy peak loads. The concept explored in this work is the benefit of combining different realistic load profiles in order to develop a total profile that is smoother and less costly to satisfy with an RER microgrid.

2. Building energy demand model

The residential load profile used for this work is generated from measured aggregate hourly consumption data for 12 apartments in a residential building in Columbus, Ohio [8]. The apartments are on the third floor of a three-story building, which means that they will have higher heating loads in the winter and cooling loads in the summer. This choice represents a worst-case scenario in terms of the peaks in the residential load. One year of hourly metered power use for these apartments is available, starting at 12 am on Sunday, June 9, 2013. These apartments use electricity for hot water, heating, and cooling. The hourly commercial load profile is synthesized from typical load profiles for commercial kitchens [9]. The average demand from the commercial load is selected to be nearly the same as the average demand from the 12 residential apartments.

2.1. Historical residential demand

Figure 1 illustrates the weekly average for the aggregate residential load data. Each day of the week, there is a peak in the morning at about 8 am, representing the electricity consumption as residents prepare for the workday. At the end of the day, at about 8 pm, there is a larger peak as residents return home for dinner and other electricity-consuming activities.

To determine the temperature-dependent component of the residential data, a piecewise linear regression is used. Each week, aggregate residential consumption data are averaged to create 52 single values. The same is done for the temperature. **Figure 2** shows a plot of the average weekly power versus average weekly outdoor temperature. The fit shown in **Figure 2** has five parameters as follows: a heating slope (HS), cooling slope (CS), heating temperature (HT), cooling temperature (CT), and baseline (B) [8]. The baseline component defines the hourly expected weather independent demand. The heating and cooling slopes KW per Fahrenheit degree (kW/°F) enable respective prediction of the hourly heating and cooling demand for a typical weather year.
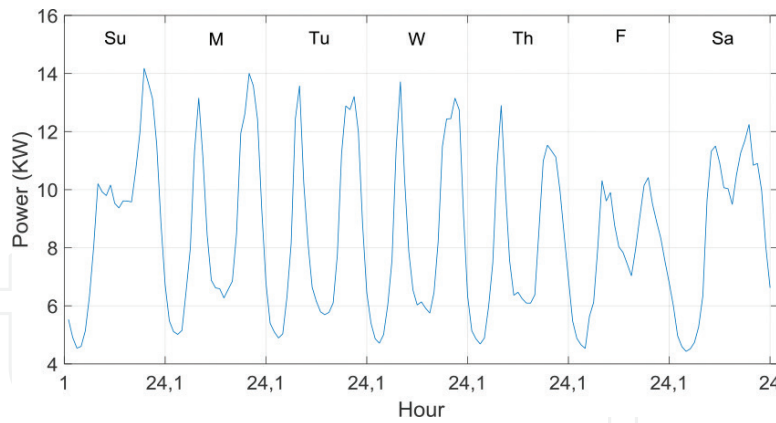
Figure 1. Weekly average aggregate residential load.

The threshold temperatures and heating/cooling slopes depend on many factors, such as building construction and size. Values for the temperature-dependent five-parameter model were calculated to be: HS = 0.16 kW/°F., CS = 0.12kW/F°, HT = 57 F°, and CT = 48 F°.

2.2. Commercial kitchen demand model

Figure 3 illustrates the weekly average baseline consumption for the commercial kitchen. The same basic profile shape is used for each day, scaled to represent the different amounts of customer traffic for each day of the week. The peak consumption occurs at 8 pm as the kitchen serves dinner, and there is also a peak at 1 pm for lunch. The kitchen uses power more consistently than the residential load through the afternoon hours.

2.3. Controlling load profile characteristics

In order to compare the three individual loads, the load factor (LF) is used. LF is defined as the ratio of the average per-month consumption to the peak hourly consumption for that month.
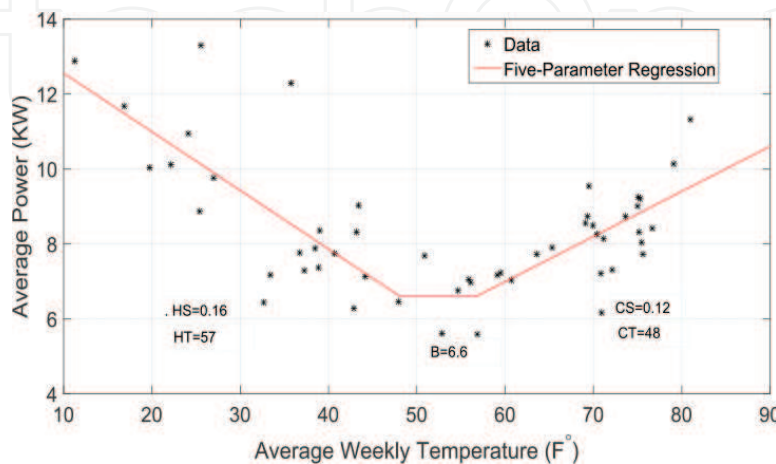

Figure 2. Temperature dependence for residential data, along with a five-parameter fit.
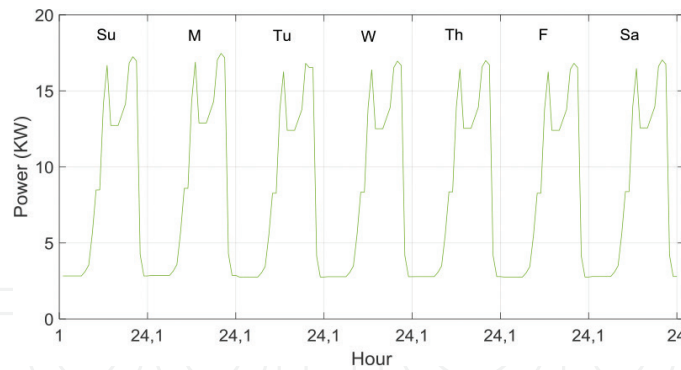
Figure 3. Weekly average commercial load (baseline).

For the data used in this study, an average yearly LF is found by averaging the 12 monthly LF values. **Figures 4** and **5** show the comparison of the monthly LF values for the three types of loads considered: residential, commercial, and combined. **Figure 4** shows the effect of combining the residential load with only the baseline commercial load. In this case, the load factor of the combined is between the residential and commercial load factors each month. **Figure 5**
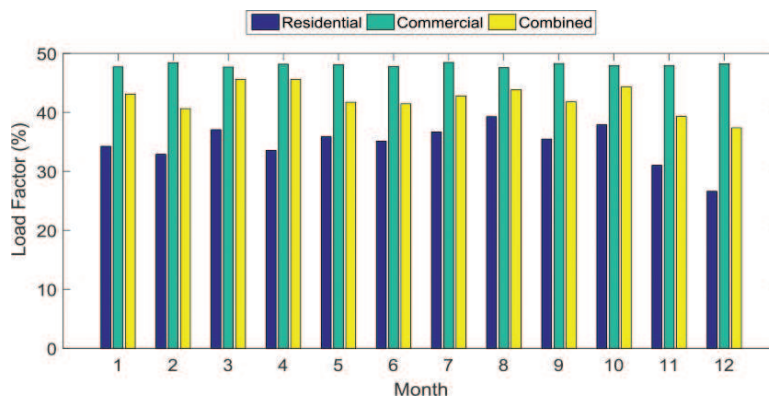

Figure 4. Comparison of monthly load factors for the three loads with no weather-dependent component.
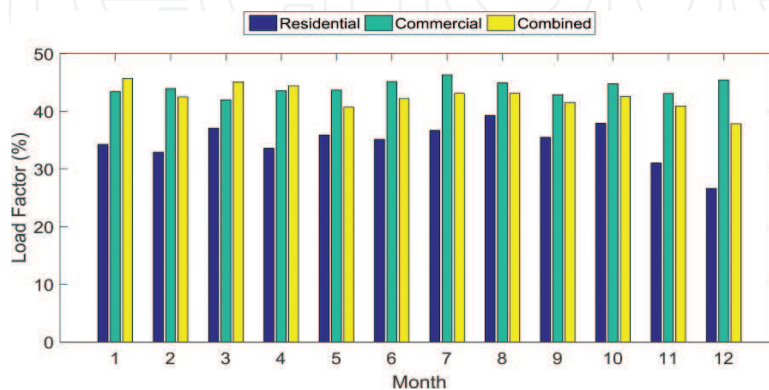

Figure 5. Comparison of monthly load factors for the three loads with weather-dependent component.

shows the effect of combining the residential load with the commercial load, where the weather-dependent load is included with the commercial load. The load factor behavior varies more in this case. The LF for the combined load is still between the LF for the residential and commercial loads, except for January, March, and April.

3. Proposed microgrid structure

The main components of the renewable energy resource (RER) microgrid examined here are solar photovoltaics (PV), micro-wind turbines (MT), and a battery energy storage system (BESS). These are utilized for electricity generation and energy storage, and they supply energy to a load that is normally satisfied with grid power alone. The microgrid is studied for two types of operating conditions. First is an isolated RER which provides all of the load power. The second system is an RER with a diesel generator backup in which the generator is activated if the RER cannot supply the full load.

For each system, the hourly power flow to or from each element of the microgrid is simulated. The capacity of each RER component is chosen to minimize the overall cost.

3.1. Isolated RER

The first type of microgrid is the isolated RER, which is shown in **Figure 6**. The RER operates independently from the local utility grid to provide all of the electricity to residential and commercial building. This system requires large battery storage to use during low wind and solar output times. The RER for the isolated mode must be large enough to produce energy to cover 100% of the building's energy needs.

3.2. RER and diesel generator

Figure 7 illustrates the second configuration and RER with a diesel generator backup. The diesel generator has the option of charging the battery, which is significantly different from the other scenarios.
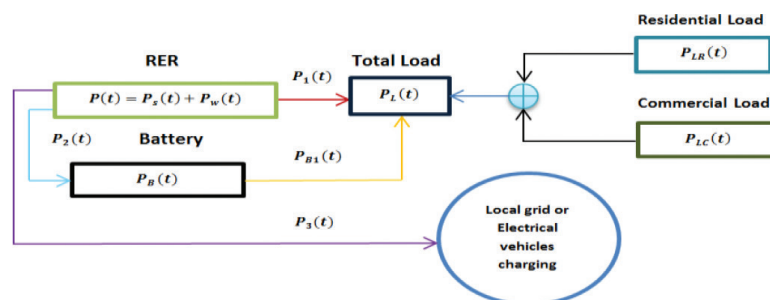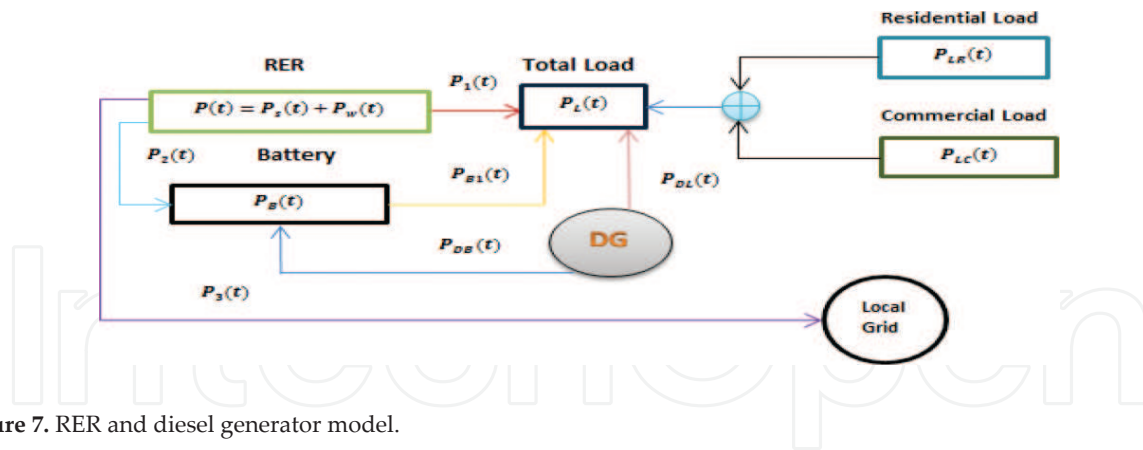

Figure 6. Isolated grid model.

Figure 7. RER and diesel generator model.

3.3. RER and battery modeling

3.3.1. Photovoltaic model

The power generated by a photovoltaic panel depends on two fundamental parameters: the solar irradiation and the ambient temperature. In order to simplify the model, the power produced by a PV panel, the following equation is used [8].

$$P_s(t) = \eta_s A_s G(t) \tag{1}$$

where η_s: Energy conversion efficiency (%), A_s: PV panel area (m²), $G(t)$: Solar irradiation (W/m^2), and $P_s(t)$: Power generated by solar PV (W).

The solar irradiation, sampled hourly, is found from typical meteorological year (TMY) data, for Columbus, Ohio [10]. The number of solar PV panels is N_s.

3.3.2. Micro-wind turbine model

The electrical power generated by a micro-wind turbine depends on the wind speed, air density, area swept by the turbine blades, and an efficiency factor called the Betz coefficient [9]. A constant air density of 1.225 k_g/m³is used, and the Betz coefficient is taken to be 59%.

$$P_w(t) = 0.5\rho A_w C_p V_w^3(t) \tag{2}$$

where ρ: Air density (k_g/m³), A_w: Micro-turbine swept area (m²), C_p: Betz coefficient, $V_w(t)$: Wind speed (m/s), and $P_w(t)$: Power generated by micro-turbine (W)

The wind speed, sampled hourly, is found from typical meteorological year (TMY) data, for Columbus, Ohio [10]. The number of micro-turbines is N_w.

3.3.3. Battery energy storage model

Whenever the RER output exceeds the load demand, the extra power is stored in a battery. This power is then used whenever the RER is unable to supply the load demand. The charge level of the battery is $P_B(t)$, which is restricted to be in the range of 20–80% of the battery capacity, B_{cap} (kWh).

$$0.2\,B_{cap} \leq P_B(t) \leq 0.8\,B_{cap} \tag{3}$$

When charging or discharging the battery, the maximum amount of energy that can be removed during a 1-hour interval is B_{HR}. This limit is expressed by the following inequality.

$$\left| P_B(t) - P_B(t-1) \right| \leq B_{HR} \tag{4}$$

Both the battery capacity and the hourly charge/discharge limit are parameters for the microgrid.

For every hour in the simulation of the microgrid, there is a decision made to charge or discharge the battery. This decision is determined in part by the charge level of the battery. If the current charge level is in the range of 20–80% of B_{CAP}, then the battery can be charged or discharged. If the current charge level is less than 20% of B_{CAP}, the battery can only be charged. If the current charge level is more than 80% of B_{CAP}, the battery can only be discharged.

3.4. Diesel generator model

The diesel generator supports the microgrid by supplying power $P_{DL}(t)$ directly to the load and power $P_{DB}(t)$ to the battery. The sum of these two must be less than the maximum power output D_{max} from the generator, such that.

$$0 \leq P_{DB}(t) + P_{DL}(t) \leq D_{max} \tag{5}$$

The conditions for activating the generator at each hour are determined by the current load and RER output, the state of the battery's charge, and whether or not the generator was running the previous hour. If the RER and battery cannot meet the load, the generator is activated. If the generator was running the previous hour and the battery can take more charge, then the generator is allowed to run during the current hour.

4. Dynamic microgrid modeling

4.1. Isolated RER dispatch algorithm

At each hour of the simulation for the grid-isolated system illustrated in **Figure 6**, the RER power $P(t)$ is determined using the TMY data. In addition, the load $P_L(t)$ and the charge level of the battery at the previous hour $P_B(t-1)$ are known. From this information, the graph in **Figure 8** is used to determine all other quantities. The graph illustrates the process of updating these quantities each hour. The following characteristics are implemented in this graph.

- If the RER output is less than the load at a given hour, then all of the available RER output is sent to the load (i.e., no battery charging at this hour), and the battery satisfies the remainder of the load.

- If the RER output is greater than the load, then the load is completely satisfied by the RER, and no battery power is used for the load. As much charging power as possible is transmitted to the battery, if its charge level is less than the upper threshold. Any remaining power from the RER is sent back to local grid.

- There is a possibility of power outage if the combined RER and battery outputs cannot meet the load. Increasing the size of the system reduces this possibility.

4.2. Diesel generator RER dispatch algorithm

At each hour of the simulation for the RER with distributed generation (DG) system illustrated in **Figure 7**, the RER power $P(t)$ is determined using the TMY data. In addition, the load $P_L(t)$ and the charge level of the battery at the previous hour $P_B(t-1)$ are known. From this information, the graph in **Figure 9** is used to determine all other quantities and to determine when the DG is turned on/off. The graph illustrates the process of updating these quantities each hour. The following characteristics are implemented in this graph.
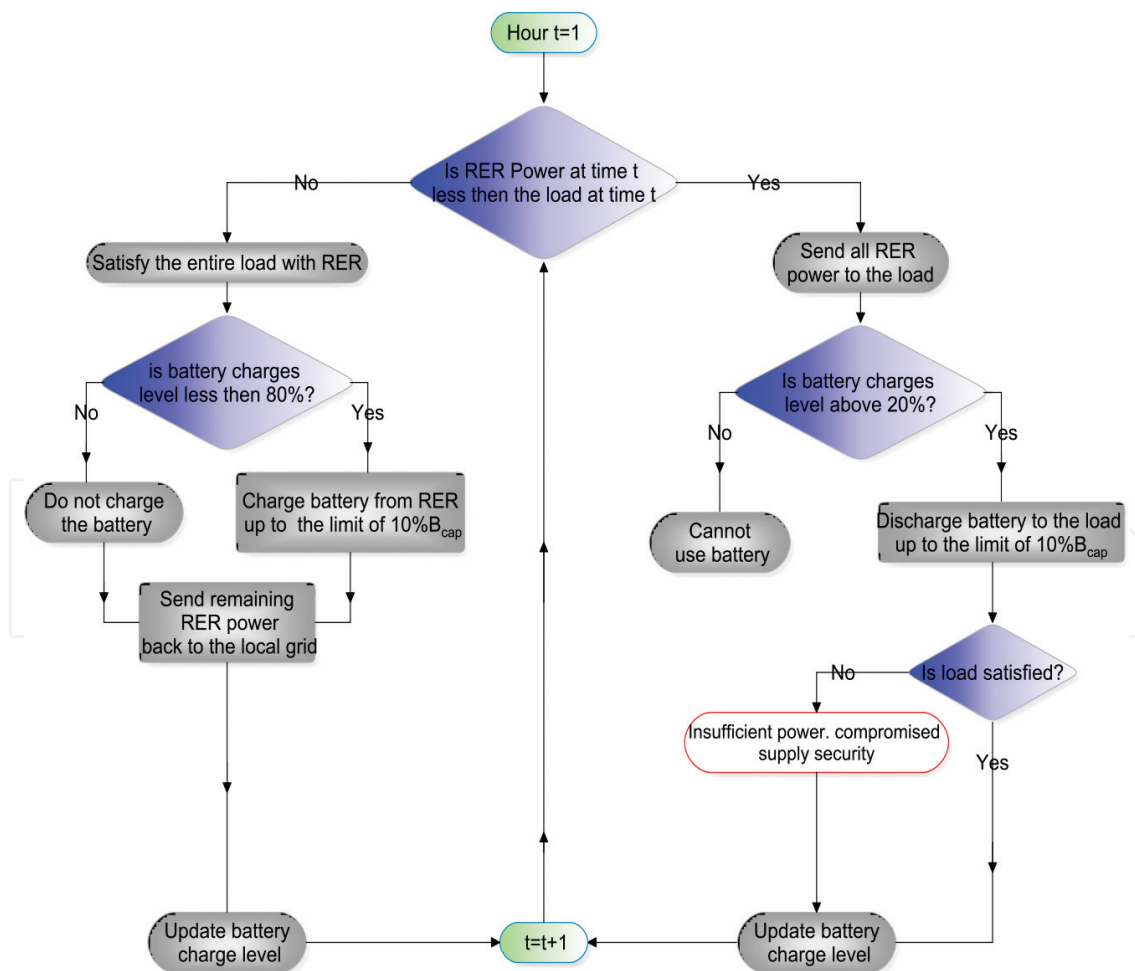

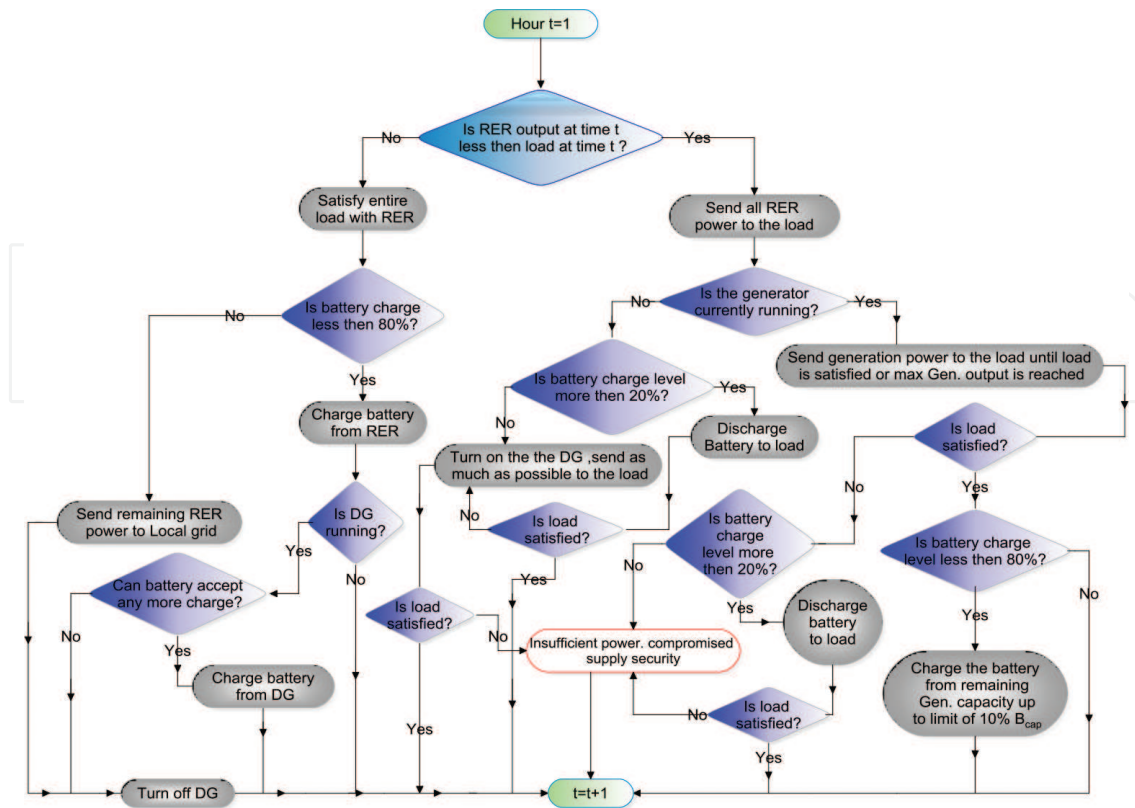**Figure 8.** Isolated RER dispatch algorithm.

Figure 9. Diesel generator RER dispatch algorithm.

- If the RER output is less than the load at a given hour, then all of the available RER output is sent to the load (i.e., no battery charging at this hour), and as much power as possible from the battery is used to meet the load if its charge level is above the minimum threshold. If this is not sufficient to meet the load, the generator is used to make up the difference.

- If the RER output is greater than the load, then the load is completely satisfied by the RER and no battery power is used for the load. As much charging power as possible is transmitted to the battery if its charge level is less than the upper threshold. Any remaining power from the RER is sent back to the local grid.

- The generator is turned on if the combined RER and battery power cannot meet the load. If it is already running, then it will remain on until the battery is fully charged.

- There is a possibility of power outage if the combined RER, battery, and DG outputs cannot meet the load. Increasing the size of the system reduces this possibility.

5. Annual cost model

The annual cost of the system, A_{CS}, is found with the following equation.

$$A_{CS} = A_{CC} + A_{RC} + A_{OC} + A_{GC} \tag{6}$$

where A_{CC} = capital cost, A_{RC} = replacement costs, A_{FC} = fuel cost, and A_{OC} = operating costs.

Each of these categories is described in the following subsections.

5.1. Annual capital cost

The capital cost is found from the initial costs for the PV array, MT units, BESS, and DG. The PV capital cost is $1.8 per peak watt of PV power. It is assumed that each solar panel in the array is 2 m² with a 20% efficiency, and that the peak radiation intensity is 1000 W/m². This leads to a per-panel capital cost of $720, with N_s panels in the entire array. Each MT unit has an up-front cost, including installation, of $22,000 (about $2 per peak watt of wind power) [11, 12]. There are N_W of these units installed. Each kWh of BESS capacity has a cost of $300 [11, 12], and the DG cost is approximated by a linear function of the capacity D_{max}, from $7000 for a 5 kW capacity to $14,000 for a 40 kW capacity, based on advertised prices [12]. The DG cost formula is therefore

$$C_{DG} = \left(D_{max} - 5 \text{ kW}\right)\left(\frac{\$7000}{35 \text{ kW}}\right) + \$7000 \tag{7}$$

The total up-front capital cost is then the sum of all four terms.

$$C_{CAP} = \$720 \cdot N_s + \$22,000 \cdot N_W + \$300 \cdot B_{Cap} + C_{DG} \tag{8}$$

Standard amortization is applied to this capital cost, using an interest rate of i = 6% and a project lifetime of N = 20 years. The amortization factor is.

$$CRF = \frac{i(1+i)^N}{(1+i)^N - 1} \tag{9}$$

This factor is applied to the capital cost to find the annual capital cost as.

$$A_{CC} = CRF \cdot C_{CAP} \tag{10}$$

5.2. Annual replacement cost

The PV and MT components last the full lifetime of the system, but the BESS and DG have shorter lifetimes and therefore need periodic replacement. Replacement costs are found with a sinking fund factor, which computes the amount of money that needs to be annually set aside to pay for periodic replacement of the BESS and DG. The formula for the sinking fund factor is.

$$SFF(N_L) = \frac{i}{(1+i)^{N_L} - 1} \tag{11}$$

The lifetime of the component in question is N_L and the interest rate i is the same as that used in the capital recovery factor. The BESS lifetime is 7 years, and the DG lifetime is 15 years. The annual replacement cost is therefore given by.

$$A_{RC} = \$300 \cdot B_{Cap} \cdot SFF(7) + C_{DG} \cdot SFF(15) \tag{12}$$

5.3. Annual operating costs

The only component that has significant operating costs is the DG, which requires fuel, oil for lubrication, and periodic maintenance. Each kWh of output from the DG requires 0.13 gallons of diesel fuel at a cost of $2 per gallon, with an additional maintenance cost of $0.05/kWh. The simulation produces the hourly output from the DG as $P_D(t)$, and summing this quantity gives the yearly energy output. For the entire plant lifetime, the total operating cost T_{OC} can therefore be given as follows.

$$T_{OC} = N \sum P_D(t) \left(0.13 \frac{\text{gal}}{\text{KWh}} 2 \frac{\$}{\text{gal}} + 0.05 \frac{\$}{\text{KWh}} \right) \tag{13}$$

This quantity can be amortized using the same amortization factor that was applied to the capital cost. This gives an annual operating cost of.

$$A_{OC} = T_{OC} \cdot CRF \tag{14}$$

6. Optimization problem formulation

In this section, the objective function is the total annual microgrid cost A_{CS} as described in the previous section. This total annual cost is a nonlinear function of the parameters N_s, N_w, and B_{CAP}, and evaluating this function requires execution of the dynamic model.

The nonlinear minimization is achieved with either the particle-swarm optimization (PSO) algorithm or the genetic algorithm (GA). PSO is used in situations in which no nonlinear constraints are needed, while GA is used if there are constraints.

Some of the constraints are simply bounds on the variables. The minimum values for each number cannot be negative, for example, and the upper bounds are chosen to be large enough for the RER to meet a required percentage of the load. The percentage of the annual load that is met by the wind and solar energy is called the renewable energy penetration formed with the following equation:

$$PEN = \frac{\sum [P_1(t) + P_2(t)]}{\sum L(t)} \times 100\% \tag{15}$$

where P_1 is Power from RER sources, P_2 is Power from battery, and L is total load.

The system with DG backup has its own dispatch algorithm, which behaves differently than the grid-connected. This is because the DG on/off cycling incurs a maintenance cost. To avoid this, the rules for determining when to turn on and off the DG are designed to minimize the number of DG cycles. To ensure that there are no power losses, the minimum DG size is restricted to be equal to the peak load, such that the DG is capable of supplying the entire load with no RER assistance, if necessary. A nonlinear constraint is used to enforce a minimum RER penetration. The optimization requires the GA, and it is summarized as follows:

$$\begin{aligned}
&\min_{N_s, N_w, B_{CAP,D_{MAX}}} A_{CS} \\
&LB_S \leq N_s \leq UB_S \\
&LB_W \leq N_w \leq UB_W \\
&LB_B \leq B_{CAP} \leq UB_B \\
&LB_{DG} \leq D_{MAX} \leq UB_{DG} \\
&PEN \geq PEN_{MAX}
\end{aligned} \tag{16}$$

where N_s is the number of solar panels, N_W is number of wind turbines, and B_{CAP} is battery capacity and diesel generation capacity.

The grid-isolated system with no backup is similarly optimized, except that the renewable energy penetration is naturally 100% for this system, since there is no diesel generator backup power used. A modified version of the backup code is used to model the grid-isolated system with no backup. To ensure that there are no power losses, the cost function includes a large cost penalty for each hour of power shortage. With this arrangement, there is no nonlinear constraint function, such that the PSO algorithm can be used. The optimization algorithm chooses a sufficiently large RER system in order to avoid the high cost penalty on the power losses.

7. Simulation results

The MATLAB simulation results for the optimization are presented in this section, for two versions of the microgrid: grid-isolated with no backup, and grid-isolated with diesel backup. The hourly RER power is generated in the same way for two cases, using hourly TMY profiles for solar radiation and wind speed. **Figure 10** shows an example of the RER power, for 10 wind turbines and 100 solar panels, relative to the combined commercial and residential load. The upper plot in this figure shows hourly RER power produced for the entire year, and the lower figure compares the RER power to the load for 1 week. When RER power output is greater than the load, the excess production can be passed to the battery. When the RER power is less than the load, the battery must make up the deficit completely for the grid-isolated with no backup scenario. If the backup is available, then these elements can be used in addition to the battery.

7.1. Isolated microgrid with no backup

The dynamic modeling results for the isolated microgrid with no backup are illustrated in **Figure 11**. This figure shows the hourly flows of power from the RER directly to the load, along with the power from the battery to the load. The RER and battery sizes must be large enough to meet the load each hour, and the figure illustrates that the combined RER and battery flows are equal to the load. This constraint forces the RER and battery sizes to be large enough to meet the highest demand in the year, which means that during most of the year the battery is not fully utilized. This fact is demonstrated by **Figure 12**, which shows the battery
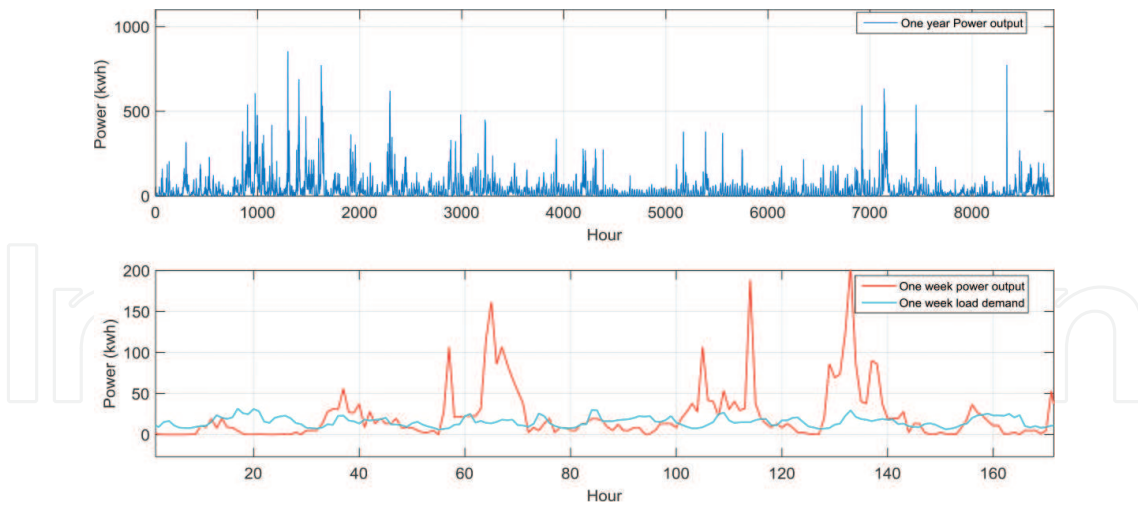
Figure 10. Combined PV and MT output for N s = 100 and N w = 10 (top). Comparison between total PV and MT output and the combined load for 1 week (bottom).
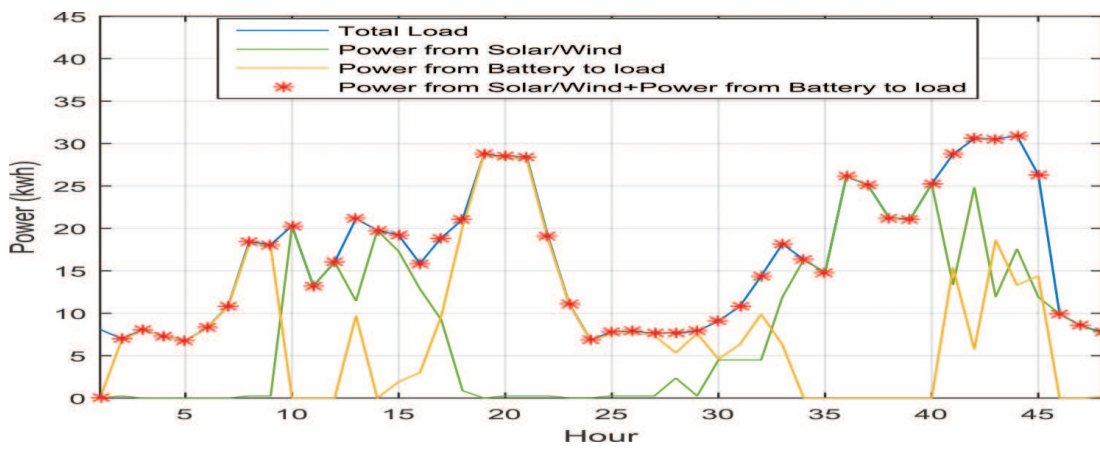

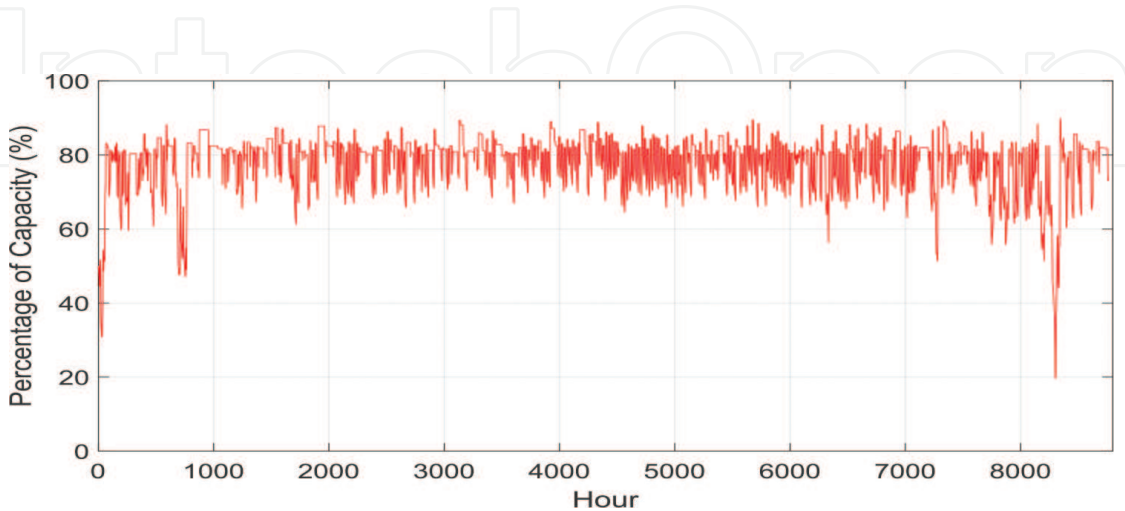**Figure 11.** Power dispatching for 48 h in January (grid-isolated no backup).

Figure 12. Battery storage level for isolated microgrid without backup.

charge level. The charge level remains high for most of the year, dipping down to low values only during a few times of peak demand.

Table 1 summarizes the results that optimize total microgrid annual cost for the residential load alone, the commercial load alone, and the mixture of the two. For comparison, the sum of the results for the residential and commercial loads is included.

When added separately, the sum of the residential and commercial load annual costs is $91,320. If these loads are mixed, however, and are satisfied by a single, larger microgrid, then the annual cost decreases to $86,000. This illustrates the cost advantage of combining the two loads into a single mixed load. Separately supplying the two loads would require more solar panels and a significantly larger battery capacity than supplying the mixed load, although the number of MTs remains the same. Because this simulation does not have diesel generator backup, the RER penetration is 100%. For each case, only about 25% of the RER output is transmitted to the load. This low percentage is due to the fact that the RER size must be chosen significantly large to meet peak yearly demand. This means that there will be many hours of energy overproduction that cannot be utilized.

7.2. Microgrid with diesel generator backup

When the grid-isolated microgrid is augmented with a DG backup system, this allows the relatively few hours of peak demand to be partially met with DG power. When the system is cost optimized, this leads to several interesting features. The size of the RER shrinks significantly, the usage of the battery becomes more regular throughout the year, and the percentage of RER power that makes it to the load nearly doubles. The trade-off for these improvements is a reduced RER penetration.

Figure 13 illustrates the power dispatching for a one-week period in January, showing the intermittent operation of the DG. The DG operates during unusually high loads, which can be seen to occur as shown in **Figure 14** when the battery energy level dips to low levels.

The DG removes the burden of meeting the peak loads from the battery, such that the energy levels in the battery can swing more uniformly over its full range throughout the year. This is illustrated in **Figure 14**, which shows the battery energy level together with the DG operation for the entire year of the simulation. The pattern in the DG clearly shows a seasonal component, such that it operates more frequently during the heating and cooling seasons.

Load		N_s	N_w	B_{CAP} (kWh)	cost (×1000 $)	%RER output to the load	%RER Pen.
No backup	Residential	388	6	621	46.20	28	100
	Commercial	428	7	487	45.12	24	100
	Sum	816	13	1108	91.32	26	100
	Mixed	790	13	959	86.00	27	100

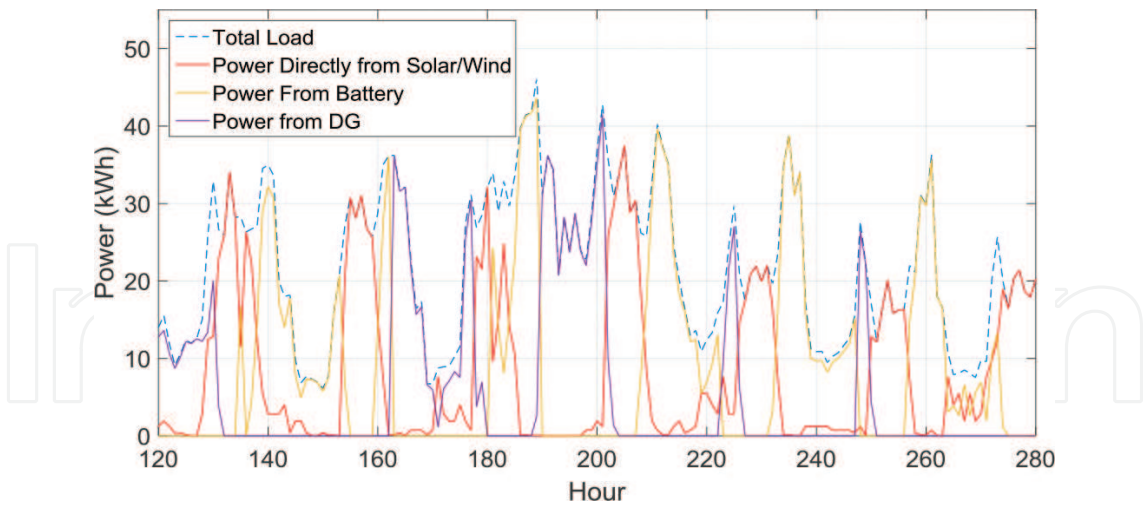**Table 1.** Optimization results for the isolated microgrid with no backup power.

Figure 13. Power dispatching for 160 h in January (grid-isolated with DG backup).
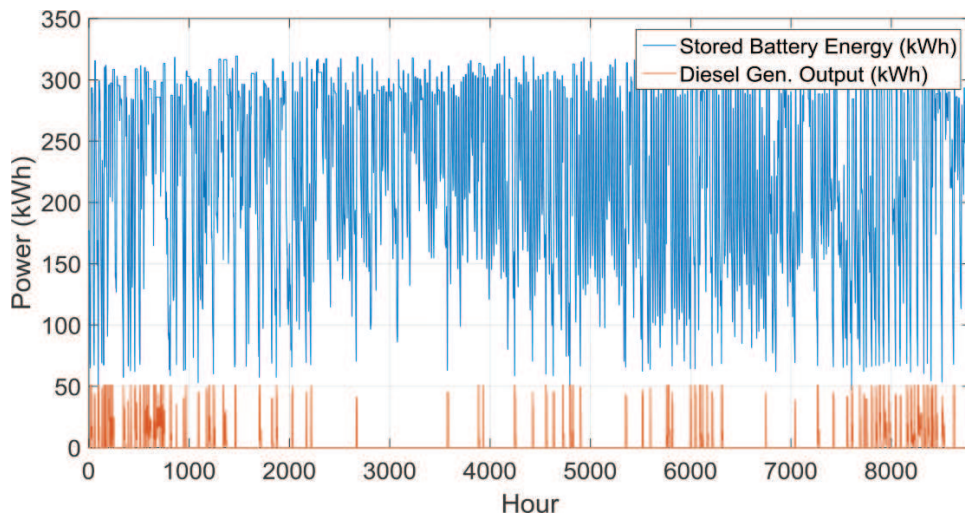

Figure 14. Battery and DG operation for microgrid with backup.

Table 2 summarizes the results that optimize total microgrid annual cost for the residential load alone, the commercial load alone, and the mixture of the two. The sum of the individual results for the residential and commercial loads is included as before, for comparison with the mixed-load results.

The largest effect of adding the DG backup to the microgrid is with the costs, which are about a fourth of the costs for the no-backup case. The optimization was made with the constraint of greater than 80% RER penetration, and it should be mentioned that the costs can be further reduced by lowering this constraint. Another large benefit in having the DG is the increase in the amount of RER power that makes it to the load, which doubles from roughly 25–50%. When comparing the sum of the costs of the residential and commercial loads to the cost of the mixed load, there is less of a difference than with the no-backup case. This indicates that the DG is reducing some of the benefit of mixing the loads.

Load	N_s	N_w	B_{CAP} (kWh)	D_{MAX} (kW)	DG on time (hr)	DG Starts	cost (×1000 $)	% RER output to the load	% RER Pen.
Residential	214	2	228	35	588	67	21.00	49	82
Commercial	244	1	215	24	756	50	20.13	47	84
Sum	458	3	443	59	1344	117	41.13	48	83
Mixed	404	1	356	50	602	83	39.68	52	82

Table 2. Optimization results for the isolated microgrid with DG backup power.

8. Summary and discussion

To illustrate the effect of renewable energy penetration, the cost optimization is constrained to produce a result with a fixed penetration. This applies to the isolated grid with diesel backup. **Figure 15** shows a plot of cost per kWh versus penetration, under the assumption that the microgrid's non-renewable power component has a price of $0.2/ kWh. Plots of the average cost per kWh for all three loads (residential, commercial, and mixed) are shown, where the average cost is computed by dividing the annual cost by the total annual load. As the renewable energy penetration approaches 100%, the cost of power from the microgrid becomes rapidly more expensive, approaching the case 1 result. As the renewable energy penetration decreases to zero, the cost of power approaches the price of nonrenewable energy, $0.2/kWh. The minimum cost per kWh occurs in the range of 30–40% of penetration.

Figure 15 also shows the interaction between load mixing and renewable energy penetration. Below 70% penetration, the mixed load cost is between the residential and commercial costs. Above this threshold, however, the mixed load cost is below both the residential and commercial costs.
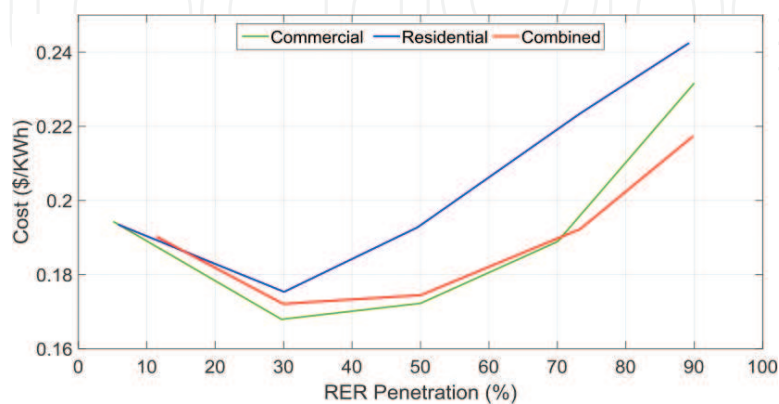

Figure 15. Average cost per kWh versus RER penetration.

9. Conclusion

The simulation results confirm that using a backup power source to support renewable energy reduces overall microgrid costs. For example, using a DG backup lowers the renewable energy penetration from 100 to 82%, but cuts the overall cost by more than a factor of two. However, the simulation results also indicate a clear benefit to mixing residential and commercial loads, such that the cost for satisfying the mixed load is less than the sum of the costs for the loads individually. Depending on the configuration, the cost for the mixed load is 3–8% less than the sum of the individual costs.

Microgrid designs for building applications involve determining the best mix of building loads for optimizing energy delivery. The result of the modeling work presented here is that combining loads allow for a measure of control over the microgrid costs. This concept is important for moving toward 100% renewable energy penetration.

Author details

Ibrahim Aldaouab* and Malcolm Daniels

*Address all correspondence to: aldaouabi1@udayton.edu

University of Dayton, Dayton, OH, USA

References

[1] Distributed Generation. Definitions, benefits, technologies & challenges. International Journal of Science and Research (IJSR). 2016;**5**(7):1941-1948

[2] How Electricity Is Delivered To Consumers. Available from: https://www.eia.gov/energyexplained/index.cfm?page=electricity_delivery [Accessed: November 7, 2017]

[3] Obi M, Bass R. Trends and challenges of grid-connected photovoltaic systems—A review. Renewable and Sustainable Energy Reviews. 2016;**58**:1082-1094

[4] Kumar Y, Ringenberg J, Depuru S, Devabhaktuni V, Lee J, Nikolaidis E, Andersen B, Afjeh A. Wind energy: Trends and enabling technologies. Renewable and Sustainable Energy Reviews. 2016;**53**:209-224

[5] Diouf B, Pode R. Potential of lithium-ion batteries in renewable energy. Renewable Energy. 2015;**76**:375-380

[6] Erdinc O, Uzunoglu M. Optimum design of hybrid renewable energy systems: Overview of different approaches. Renewable and Sustainable Energy Reviews. 2012;**16**(3):1412-1425

[7] Shaahid SM, Elhadidy MA. Technical and economic assessment of grid-independent hybrid photovoltaic–diesel–battery power systems for commercial loads in desert environments. Renewable and Sustainable Energy Reviews. 2007;**11**(8):1794-1810

[8] Aldaouab I, Daniels M, Hallinan K. Microgrid Cost Optimization for a Mixed-Use Building. In: 2017 IEEE Texas Power and Energy Conference (TPEC). 2017

[9] Aldaouab I, Daniels M. Microgrid battery and thermal storage for improved renewable penetration and curtailment. In: IEEE International Energy & Sustainability Conference (IESC). 2017

[10] NSRDB Update—TMY3: Alphabetical List by State and City. Available from: http://rredc.nrel.gov/solar/old_data/nsrdb/1991-2005/tmy3/ [Accessed: December 1, 2017]

[11] Aldaouab I, Daniels M. Renewable energy dispatch control algorithms for a mixed-use building. In: 2017 IEEE Green Energy and Smart Systems Conference IGESSC. 2017

[12] Find Quality Manufacturers, Suppliers, Exporters, Importers, Buyers, Wholesalers, Products and Trade Leads from OurAward-winning International. Available from: http://https://www.alibaba.com [Accessed: February 2, 2017]